INTERNATIONAL JOURNAL OF CLIMATOLOGY
Int. J. Climatol. (2015)
Published online in Wiley Online Library
(wileyonlinelibrary.com) DOI: 10.1002/joc.4549

Changes in clustered extreme precipitation events in South China and associated atmospheric circulations

Huixin Li,[a,c] Huopo Chen[a,b]* and Huijun Wang[a,b]

[a] *Nansen-Zhu International Research Centre, Institute of Atmospheric Physics, Chinese Academy of Sciences, Beijing, China*
[b] *Collaborative Innovation Center on Forecast and Evaluation of Meteorological Disasters, Nanjing University of Information Science & Technology, China*
[c] *University of Chinese Academy of Sciences, Beijing, China*

ABSTRACT: Previous studies have documented that the summer precipitation over South China (SC) has experienced a prominent inter-decadal increase in 1992/1993, and the possible mechanism has been well revealed. The aim of this study is to investigate the changes in extreme precipitation and clustered extreme precipitation events in recent decades using station observations and the National Centers for Environmental Prediction/National Center for Atmospheric Research (NCEP/NCAR) reanalysis data. The results indicate that extreme precipitation also experienced a significant inter-decadal increase around 1992/1993. Significant changes can also be found in the associated atmospheric circulations, such as the western North Pacific subtropical high (WNPSH) and the westerly jet stream over East Asia. In addition, the water vapour transport (WVT) related to extreme precipitation differed from mean conditions. For extreme precipitation events, the WVT from the Northwest Pacific and Indian Oceans was much stronger when compared with mean precipitation. When extreme precipitation events were clustered, the increased WVT mainly originated from the South China Sea and Northwest Pacific Ocean. Further analysis indicates that the WVT increased from the Indian Ocean but decreased from the Northwest Pacific after 1992/1993; this finding explains the significant increase in the clustered extreme precipitation events over SC after 1992/1993. In addition, the atmospheric stratification has become more unstable since 1992/1993.

KEY WORDS extreme precipitation; clustered extreme precipitation; South China; water vapour transport; atmospheric stratification

Received 26 March 2015; Revised 7 September 2015; Accepted 2 October 2015

1. Introduction

The summer precipitation over eastern China has greatly changed in recent years (Zhu *et al.*, 2011). The associated extreme precipitation events (including their frequency and intensity) also experienced significant changes that varied by region and season (Zhai *et al.*, 1999, 2005; Wang and Zhou, 2005; Ding *et al.*, 2006). Previous studies have revealed that the inter-decadal pattern of summer precipitation over East China changed significantly in the late 1970s and 1990s (e.g. Ding *et al.*, 2008). The decadal shift of the precipitation pattern in the late 1970s, in which more precipitation in the Yangtze River Valley and less precipitation in northern China, is attributed to the weakness of the East Asian summer monsoon (Wang, 2001; Gong and Ho, 2002; Ding, 2007; Han and Wang, 2007; Zeng *et al.*, 2007). In the late 1990s, with the northward movement of the rain belt, the precipitation decreased over the Yangtze River but increased in the Huang-Huai region (Si *et al.*, 2009; Zhu *et al.*, 2011). Summer precipitation over South China (SC) also experienced a significant increase in the early 1990s (Wu *et al.*, 2010).

Numerous studies have revealed the possible mechanisms for the precipitation changes over East China. For example, the sea surface temperature (SST) variations in the North Pacific Ocean play an important role in the inter-decadal change in the summer precipitation pattern in East China (Chang *et al.*, 2000). In the early 1990s, summer precipitation over SC significantly increased, and the associated atmospheric circulations also presented obvious changes (Kwon *et al.*, 2005, 2007). Wu *et al.* (2010) further indicated that an increase in the Tibetan Plateau snow cover in the preceding winter–spring and the increase in the SST in the equatorial Indian Ocean are possible reasons for the increase in summer precipitation over SC.

One direct and important factor for the precipitation change is the water vapour transport (WVT) (Zhang, 2001). Huang *et al.* (2011) reported that the variations in summer precipitation anomalies over the monsoon region are closely related to variations in the WVT fluxes over East Asia. Sun *et al.* (2011) also found that the WVT induced by the East Asian and the Indian monsoons plays an important role in the changes in summer precipitation over the Yangtze and Huang-Huai River Valleys. Furthermore, the WVT induced by the East Asian

* Correspondence to: H. Chen, Nansen-Zhu International Research Centre (NZC), Institute of Atmospheric Physics, Chinese Academy of Sciences, 40# Hua Yan Li, Chao Yang District, Beijing 100029, China. E-mail: chenhuopo@mail.iap.ac.cn

monsoon is mainly contributed to meridional transport (Huang *et al.*, 1998). Another recent study (Wang and Chen, 2012) revealed that although the primary moisture source is the Indian Ocean, the basic regulations of the variations in summer precipitation in eastern China are the western North Pacific Subtropical high (WNPSH) and the East Asian summer monsoon, rather than the Indian summer monsoon. From previous studies, it is clear that these investigations of the changes in WVT mainly refer to mean conditions, while few studies consider extreme precipitation events.

SC is deeply influenced by the East Asian monsoon. Summer precipitation over this region has demonstrated an obvious inter-annual variability, as well as a significant inter-decadal variability, with an abrupt increase around 1992/1993 (Yao *et al.*, 2008; Ding *et al.*, 2009; Sun *et al.*, 2012). This increase is even larger than that in the Yangtze River region in the late 1970s (Wu *et al.*, 2010). Further analyses indicated that there is enough moisture in this region to create favourable conditions for heavy rainfall (Ding *et al.*, 2009). Similar to mean precipitation, the extreme precipitation events in SC also present a prominent increase in the early 1990s (Ning and Qian, 2009). Furthermore, some studies detected that the frequency and intensity of extreme precipitation present a clustered character due to anomalous atmospheric circulations (Qian *et al.*, 2007).

In general, the clustered extreme precipitation events can cause severe natural disasters, such as landslides and floods, which result in relatively larger economic losses than other types of extremes. The aim of this study is to investigate the changes in extreme precipitation events and clustered extreme precipitation events over SC in recent decades. The associated atmospheric circulations and WVT are further revealed. Accordingly, the structure of this article is as follows. Section 2 presents a simple introduction of the data and methods. Section 3 presents the characteristics of the changes in extreme precipitation events in SC, and Section 4 provides a discussion of the results of the clustered extreme precipitation events and associated changes in atmospheric circulations and WVT. The conclusions are provided in Section 5.

2. Data and methods

The monthly and 6-hourly mean reanalysis data sets from the National Centers for Environmental Prediction/National Center for Atmospheric Research (NCEP/NCAR) are used in this study; the data have a horizontal resolution of 2.5° × 2.5° (longitude × latitude). The variables used here include the surface pressure, meridional and zonal winds, vertical velocity, air temperature, specific humidity, and relative humidity. The 6-hourly integrated data sets from the European Centre for Medium-Range Weather Forecasts (ECMWF) Interim reanalysis (ERA-Interim) with a horizontal resolution of 1.5° × 1.5° (longitude × latitude) are also used. The variables used here include vertical integral of eastward water vapour flux, vertical integral of northward water vapour flux, and vertical integral of divergence of moisture flux. In addition, the daily precipitation data for the period 1960–2010 are available at 50 stations in SC among the 756 stations in China, as collected by the National Meteorological Information Center. The SC region is within 110°–120°E and 22.5°–27.5°N. The extreme precipitation events in this study are defined as events with daily precipitation rates exceeding 25 mm day^{-1}. Clustered extreme precipitation events are defined as events that occur over more than half sites in the SC region. In this study, we note a prominent inter-decadal shift of summer extreme precipitation events in SC around 1992/1993; thus, the analysed period is divided into 1975–1992 and 1993–2010.

The vertically integrated water vapour flux is calculated as follows:

$$Q = Q_\lambda \vec{i} + Q_\varphi \vec{j}$$

$$Q_\lambda \approx \sum_{n=n_0}^{N} \frac{1}{2}\left(q\left(p_{n+1}\right)u\left(p_{n+1}\right) + q\left(p_n\right)u\left(p_n\right)\right)\left(p_{n+1} - p_n\right) + q\left(p_{n0}\right)u\left(p_{n0}\right)\left(p_{n0} - p_s\right)$$

$$Q_\varphi \approx \sum_{n=n_0}^{N} \frac{1}{2}\left(q\left(p_{n+1}\right)v\left(p_{n+1}\right) + q\left(p_n\right)v\left(p_n\right)\right)\left(p_{n+1} - p_n\right) + q\left(p_{n0}\right)v\left(p_{n0}\right)\left(p_{n0} - p_s\right)$$

where Q_λ and Q_φ are the zonal and meridional components, respectively (Trenberth *et al.*, 2007) and n is the level. The vertical integral of water vapour flux has to be approximated following the trapezoidal rule, and the effects of the complex topography in the vertical integration of the water vapour flux have been considered. The surface pressure is used to remove the impact of the topography (i.e. the water vapour is set to zero at pressure levels below surface pressure).

In addition, the K index is calculated to analyse changes in the atmospheric stratification stability: $K = (T_{850} - T_{500}) + Td_{500} + (T - Td)_{700}$ (Chen *et al.*, 2012a). In general, a larger K index represents a more unstable atmospheric stratification, which favours convective motion in atmosphere.

It is important to note that Beijing Time (BT) is 8 hour ahead of coordinated universal time (UTC); thus, it would be more precise to use the 6-hourly mean reanalysis data sets for describing the WVT and atmospheric conditions than the daily data directly derived from NCEP/NCAR (Sun and Wang, 2013). The daily data sets are derived from 6-hourly data sets by averaging five times: 1200 and 1800 of the previous day and 0000, 0600, and 1200 of the current day.

3. Summer extreme precipitation events over SC

Figure 1 shows the locations of 50 selected stations in SC. Professional weather observers in China maintain

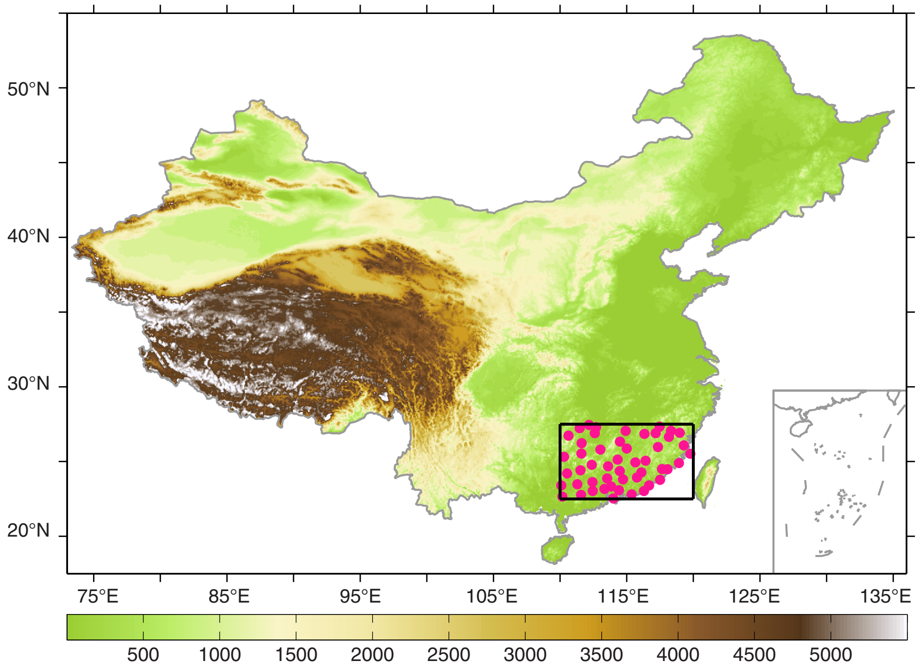

Figure 1. Maps of station locations in South China and corresponding topography (shading) in China. The black box means the region of South China. Unit: m.

these stations and the data are collected and released by the National Meteorological Information Center, as well as their homogeneity and quality control processes. In addition, there is no steep topography in this region and the stations are homogeneously distributed. To reduce the uncertainty from the different definitions of the clustered extreme precipitation, several classifications are calculated varying from the precipitation levels (including 10, 25, and 50 mm day^{-1}) and station numbers (including more than 30, 40, 50, 60, and 70% of stations over SC). Similar results can be observed from these different cases, with obvious increase and intensification for these clustered extreme precipitation events after 1993 (Table 1). Thus, the threshold of 25 mm/day with 50% stations is selected as a specific case for further analysis on the change characteristics of the clustered extreme precipitation events.

The latitude-time cross section of the 9-year filtered summer (JJA: June, July, and August) precipitation averaged over 110°–120°E in East China (figure not shown) indicates that there is a prominent increase in summer precipitation over SC since 1992/1993; this finding is consistent with previous studies. In general, the changes in the mean precipitation are mainly attributed to the changes in extreme precipitation events (Chen *et al.*, 2012b). Thus, variations in extreme precipitation over SC are first explored.

Figure 2(a) shows the proportion of extreme precipitation to summer total precipitation over SC, while Figure 2(b) shows the variations in the frequency of extreme precipitation. Obvious inter-annual variability, including frequency and intensity variations can be observed. To understand the relationship between the summer mean precipitation and the extreme precipitation, the correlation coefficients are computed. The correlations with the extreme precipitation proportion, frequency, and intensity of the extreme precipitation are 0.75, 0.70, and 0.39, respectively; all of these values are significant at the 95% confidence level. In addition, the annual amount of extreme precipitation accounts for 62% of the summer total precipitation. Thus, the variations in summer mean precipitation over SC can be mainly attributed to the changes in extreme precipitation in recent decades.

Furthermore, the extreme precipitation over SC also experienced a significant inter-decadal change in recent decades (Figure 2(c)). The result from the Mann–Kendall test for the frequency of extreme precipitation indicates that it has been increased significantly since 1992/1993. This inter-decadal shift can also be observed in the total amount and intensity of extreme precipitation. The average extreme precipitation was observed to increase by 43% from 328.4 mm per year during 1975–1992 to 469 mm per year during 1993–2010. Similarly, the proportion increased by 9% from 59.3 to 64.8%. The frequency increased by 10% from 61 to 67 occurrences, and the intensity increased by 3% from 49.8 to 51.2 mm/day.

4. Summer clustered extreme precipitation events in SC

Clustered extreme precipitation events generally lead to more direct natural disasters compared with general extreme precipitation events, and their associated atmospheric circulations and WVT are substantially different.

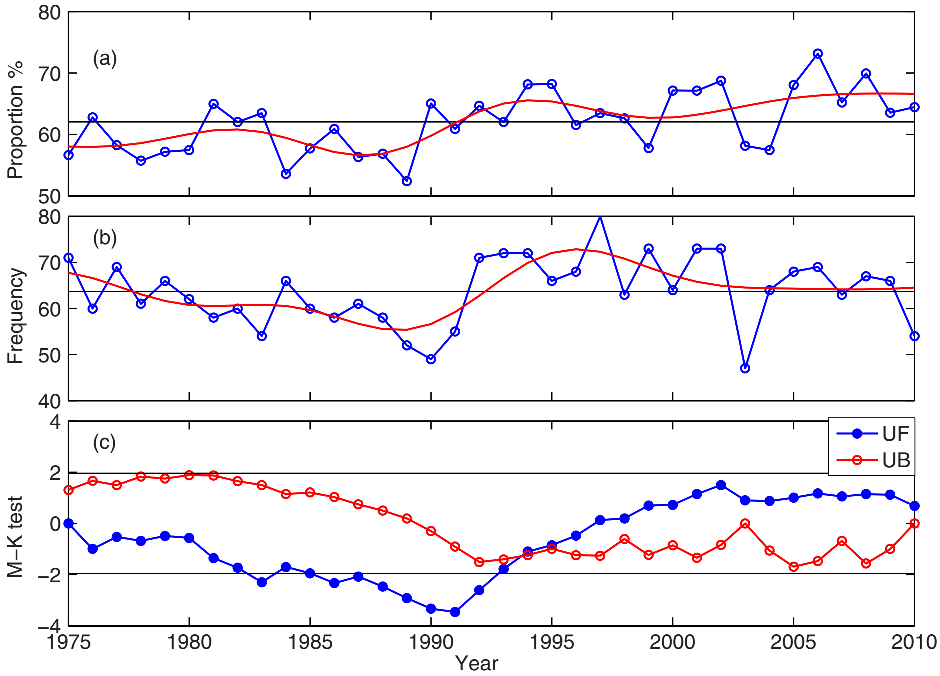

Figure 2. Variations in the (a) proportion of extreme precipitation to total precipitation, (b) frequency of extreme precipitation (blue for original variation, red for 9-year low-pass filter), and (c) Mann–Kendall test for the frequency of extreme precipitation (red line represents UB, and the blue line represents UF).

Considering the threshold of 25 mm/day with 50% stations, clustered extreme precipitation events occurred 22 times during 1975–2010, according to the definition mentioned above; 8 events occurred during 1975–1992, and 14 events occurred during 1993–2010. Further analysis indicates that the intensity of the clustered extreme precipitation events increased by 2% from 63.8 mm during 1975–1992 to 65.4 mm during 1993–2010 (Table 1). In addition, 14 cases were observed to occur in June (pre-rainy season in SC), and 8 cases occurred in July and August; thus, the clustered extreme precipitation events mainly occurred in the pre-rainy season in SC.

4.1. Meteorological conditions for the clustered extreme precipitation events

First, the meteorological conditions for the clustered extreme precipitation events over SC are explored. Figure 3(a) shows the spatial distributions of the WNPSH for different periods. In the case of clustered extreme precipitation during 1975–2010, the ridge of the WNPSH was located at approximately 18°N, which is approximately 7° south of the summer mean position. In general, the rain belt often locates 6°–10° north of the ridge of the WNPSH (Zhu, 2007); the region of SC has an increasing probability of occurrence of heavy precipitation in this case. Moreover, previous studies have documented that the meridional movement of the WNPSH is favourable for the change in meteorological conditions and that intensive precipitation would occur in the pre-rainy season over SC due to the westward shift of the WNPSH (e.g. Yang and Sun, 2005). It is clear that there is a 10° westward shift in the mean summer conditions, from 133° to 123°E.

To understand the changes in the corresponding atmospheric circulation in the upper and lower troposphere, the spatial distributions of the zonal wind at 200 hPa during 1975–2010 are shown (Figure 3(b)). As expected, changes in the zonal winds in the East Asian subtropical westerly jet (EAWJ) region ‘A’ were highly correlated with those of the summer total precipitation over SC, indicating that a weaker zonal wind in the A area corresponds to more precipitation over SC during summer. Figure 3(c) shows the difference in the zonal winds over 200 hPa between the clustered extreme precipitation events and the summer mean conditions. The results indicate a relatively weak zonal wind in the A region, suggesting an enhancement of clustered extreme precipitation over SC. In addition, the axis of the EAWJ was observed to move southward, intensifying significantly in the Yangtze River–Japan area. Du *et al.* (2008) indicated that the EAWJ core favors horizontal divergence on its right side. In this case, the zonal position of the EAWJ in the upper levels provided an intense divergent circulation over SC, inducing upward motion and an enhanced convergence centre at the lower levels. In general, the water vapour content is concentrated in the low levels, so variations in the 850 hPa circulation are documented. The result from Figure 3(e) indicates that the warm and humid airflow from the Northwest Pacific Ocean and the South China Sea provided enough moisture for the occurrence of clustered extreme precipitation over SC. Because of the southward movement of the EAWJ and the westward movement of the WNPSH, the southwest flow along the western rear of the WNPSH was enhanced, inducing a cyclonic circulation anomaly centred over SC. The above analysis indicates that the circulation

Table 1. Frequency and intensity for the clustered extreme precipitation events in different precipitation levels and different station numbers during the period 1975–1992 and 1993–2010.

Rainfall amount (≥)	Number of stations (>)	Frequency		Intensity (mm/day)		Frequency ratio	Intensity ratio
		1975–1992	1993–2010	1975–1992	1993–2010	1993–2010/1975–1992	1993–2010/1975–1992
10	15 (30%)	305	439	35.45	37.35	1.44	1.05
	20 (40%)	173	257	37.23	39.56	1.49	1.06
	25 (50%)	94	140	39.73	42.89	1.49	1.08
	30 (60%)	36	59	41.51	44.93	1.64	1.08
	35 (70%)	12	19	44.55	49.27	1.58	1.11
25	15 (30%)	57	127	60.81	59.76	2.23	0.98
	20 (40%)	21	43	61.98	63.83	2.05	1.03
	25 (50%)	8	14	63.88	65.40	1.75	1.02
	30 (60%)	2	8	57.24	67.83	4.00	1.18
	35 (70%)	0	1	–	75.77	–	–
50	15 (30%)	5	11	88.37	94.84	2.20	–
	20 (40%)	0	2	–	106.18	–	–
	25 (50%)	0	2	–	106.18	–	–
	30 (60%)	0	0	–	–	–	–
	35 (70%)	0	0	–	–	–	–

anomalies over the middle and lower latitudes were inherently connected with the occurrences of clustered extreme precipitation events over SC.

As mentioned above, the clustered extreme precipitation events over SC increased significantly after 1992/1993. The reasons for this change are unclear, and more research is needed. Thus, the circulation differences between the two periods of the clustered extreme precipitation events are explored. It can be concluded from Figure 3(a) that the average position of the WNPSH moved westward, with an enhancement of the Indian monsoon for 1993–2010 compared with that for 1975–1992. In addition, although the westward shift of the WNPSH helps increase the precipitation, it has no relationship to the inter-decadal change around 1992/1993, which agrees with the study by Kwon *et al.* (2007). In the low levels, an abnormal southerly flow from the South China Sea and the North Indian Ocean dominated SC (Figure 3(f)), indicating an enhanced role of the Indian Ocean pathway after 1992/1993. The zonal winds in the A area further weakened after 1992/1993, in conjunction with a distinct increase in clustered extreme precipitation over SC (Figure 3(d)). Meanwhile, the divergence in the upper levels increased after 1992/1993, in conjunction with the enhancement of low-level convergence over SC.

4.2. Water vapour transport

Figure 4(a) presents the vertically integrated water vapour anomaly for general extreme precipitation events over SC during 1975–2010. A cyclonic convergence anomaly dominated SC, providing sufficient moisture for extreme precipitation occurrences. Furthermore, the WVT decreased from the Indian Ocean but increased from the Northwest Pacific Ocean after 1992/1993 (Figure 4(b)). Figure 4(c) shows the anomalous WVT for clustered extreme precipitation events compared with general extreme precipitation events during 1975–2010. Differences can be observed: the WVT significantly increased, and the associated convergence intensified. In addition, the water vapour budget for each boundary around SC was computed. The southerly enhanced influxes via the south boundaries of the South China Sea, the Northwest Pacific, and the tropical Indian Ocean positively affected the clustered extreme precipitation events. Furthermore, the increased water vapour from the Northwest Pacific Ocean played a relatively more important role than that from the Indian Ocean. Meanwhile, the water vapour flux anomaly from SC via the north boundary decreased. Figure 4(d) shows the differences of the water vapour fluxes for the clustered extreme precipitation events over SC between 1993–2010 and 1975–1992, as well as the corresponding divergence and convergence. Interestingly, with the increase in clustered extreme precipitation over SC during 1993–2010, the water vapour fluxes from the tropical Indian Ocean and the South China Sea strengthened, whereas the fluxes from the Northwest Pacific Ocean weakened. The moisture budget indicates that the water vapour leaving eastern SC via its east boundary significantly decreased, and the net moisture influx over SC increased by 1.39×10^7 kg s^{-1}.

Seager and Henderson (2013) pointed out that there are some differences between the computed moisture divergence and the ERA-Interim-reported values. Thus, the ERA-Interim data sets with higher resolution are used to check results from the NCEP-1 (Figure 5). Clearly, results from the ERA-Interim are nearly the same as NCEP-1 in Figure 4. Thus, the results shown here are robust.

Figure 6(a) shows the WVT anomalies and the corresponding moisture divergence at 850 hPa for the clustered extreme precipitation events over SC during 1975–2010. Similar results can be observed from Figure 4(c), except for minor differences, namely, a cyclonic anomaly dominated SC when clustered extreme precipitation events occurred. Increased moisture was mainly supplied by the

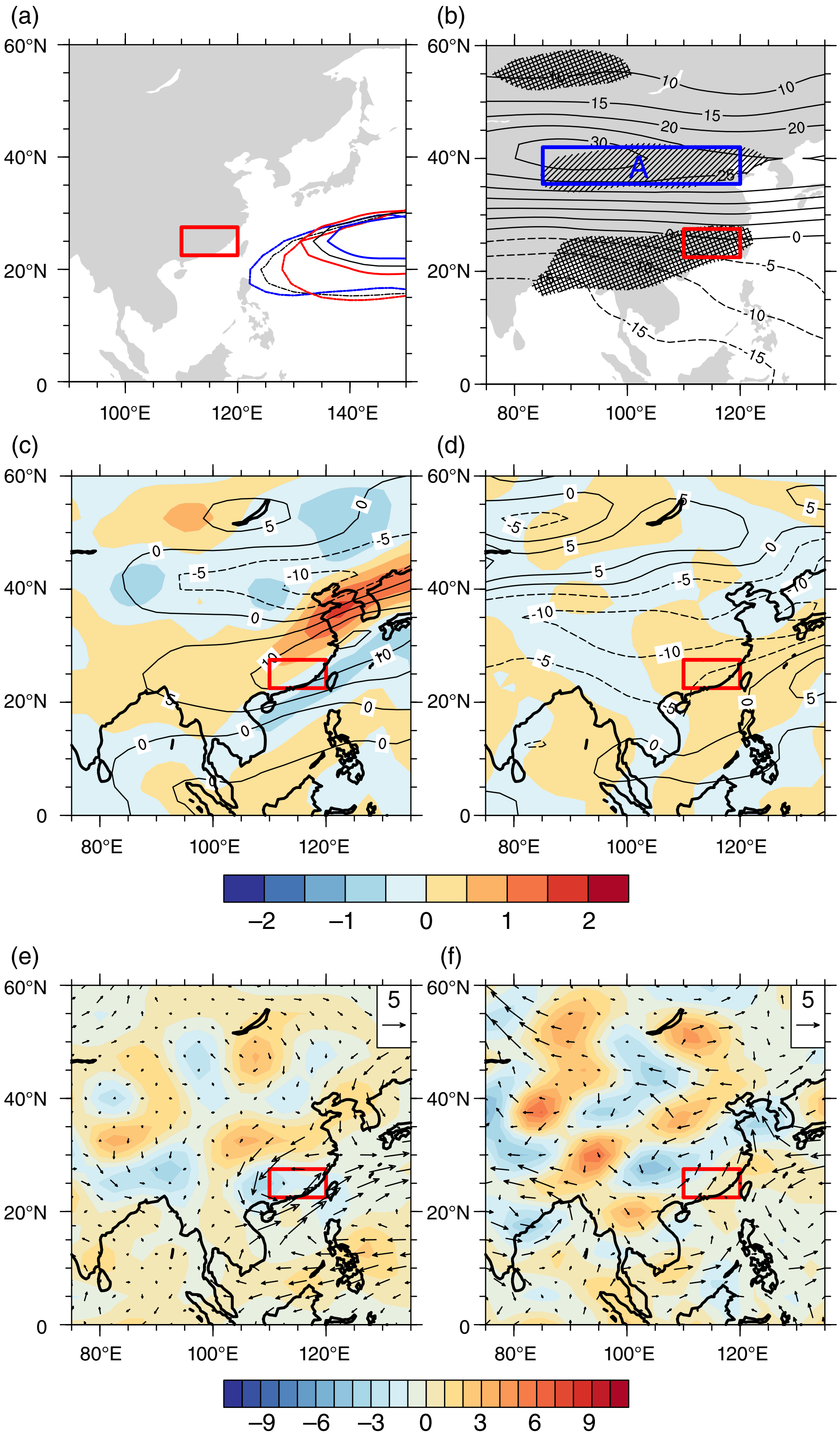

Figure 3. (a) A 5880-gpm mean position in summer at 500 hPa (the dashed lines are clustered extreme precipitation, and the solid lines are the summer mean position) during 1975–1992 (blue), 1993–2010 (red), and 1975–2010 (black); (b) the climatological 200 hPa zonal winds in summer during 1975–2010 (shading indicates the correlations between the 200 hPa zonal wind and precipitation over SC that are significant at the 95% level; the crosses are positive and oblique is negative for 'A'); (c) climatological anomaly of the 200 hPa zonal wind for clustered extreme precipitation (the units of the zonal wind are m s^{-1}; the units of divergence are 10^{-5} s^{-1}); (d) same as (c) but for the differences between two sub-periods; (e) climatological anomaly of 850 hPa wind vectors for clustered extreme precipitation (units of wind vectors are m s^{-1}; the units of divergence are 10^{-6} s^{-1}); (f) same as (e) but for the differences between two sub-periods. The red box represents the region of South China.

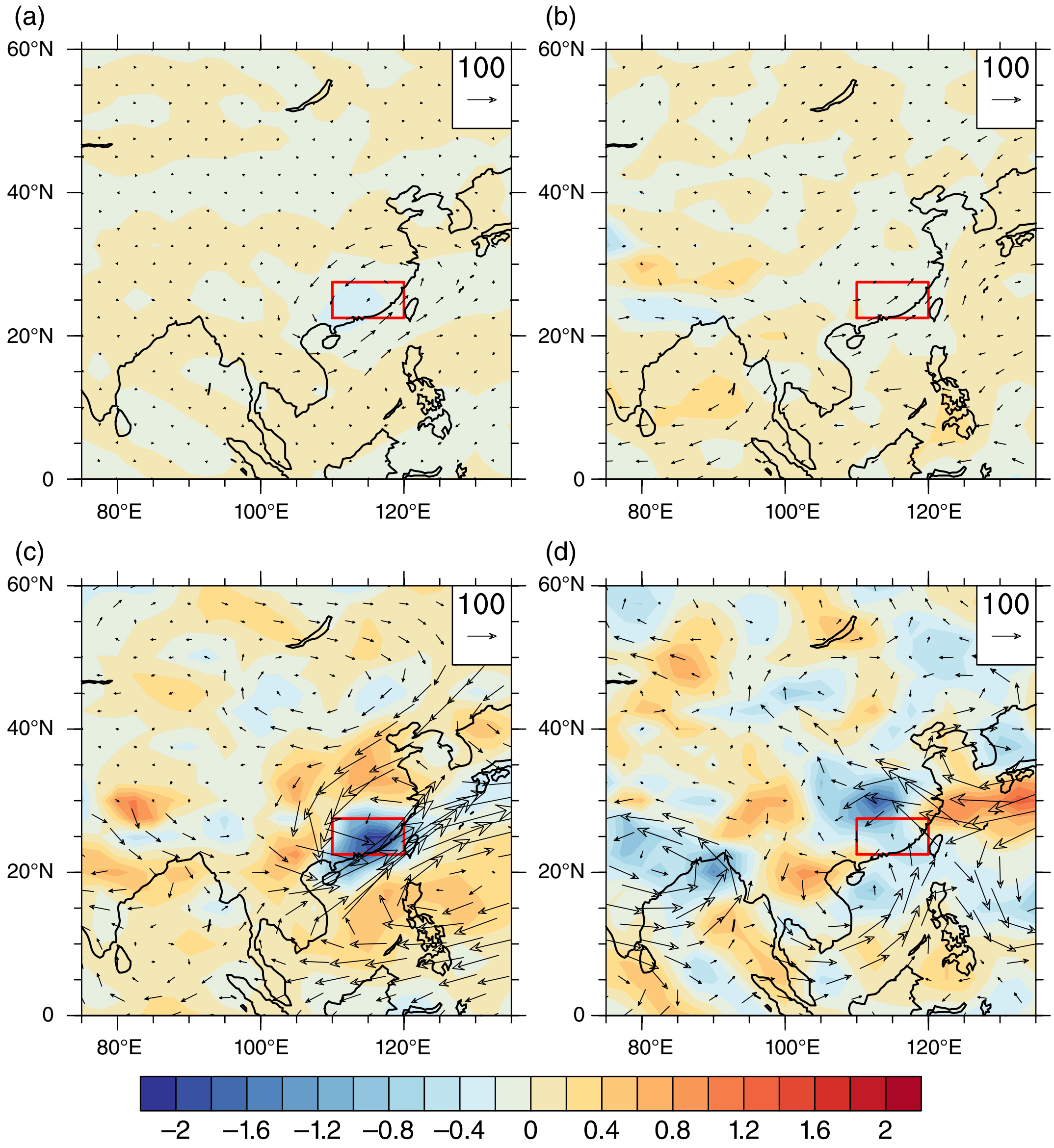

Figure 4. Spatial distributions of integrated water vapour transport anomalies: (a) anomaly for summer extreme precipitation during 1975–2010; (b) same as (a) but for the differences between two sub-periods; (c) same as (a) but for the differences between clustered and general extreme precipitation events; (d) same as (b) but for the clustered extreme precipitation events (units of water vapour transport are kg m^{-1} s^{-1}; units of divergence are 10^{-4} kg m^{-2} s^{-1}). The red box represents the region of South China.

South China Sea and the Northwest Pacific Ocean, which dominated the WVT anomaly. The tropical Indian Ocean route also played a role, but it was not as important as the previous two routes. The WVT decreased at 700 hPa because moisture decreases with height, but the characteristics were similar to 850 hPa in that the anomalous moisture from the South China Sea and the Northwest Pacific was dominant; however, the role of the tropical Indian Ocean increased (figure not shown). Figure 7(a) shows the case of 300 hPa, with a prominent westerly moisture anomaly over SC, indicating the important role of the Indian Ocean. In addition, SC was mainly dominated by a moisture divergence anomaly in the upper levels, with a convergence anomalies to the north and south; this pattern is opposite of that in the lower levels. Decadal differences in the associated WVT for the clustered extreme precipitation events were also investigated at the low levels (Figure 6(b)). Similarly, the moisture anomaly from the South China Sea and the tropical Indian Ocean strengthened during 1993–2010 but weakened from the Northwest Pacific Ocean compared with 1975–1992. This finding is consistent with the vertically integrated results. In addition, the dominant abnormal easterlies over SC in the upper levels indicate a weaker role of the Indian Ocean after 1992/1993 (Figure 7(b)).

In summary, when general and clustered extreme precipitation events occurred, the corresponding water vapour exhibited a cyclonic anomaly over SC. Compared with general extreme precipitation, the WVT into SC via the southern boundary became much stronger for clustered extreme precipitation. Moreover, the associated moisture convergence also increased over this region. A decadal

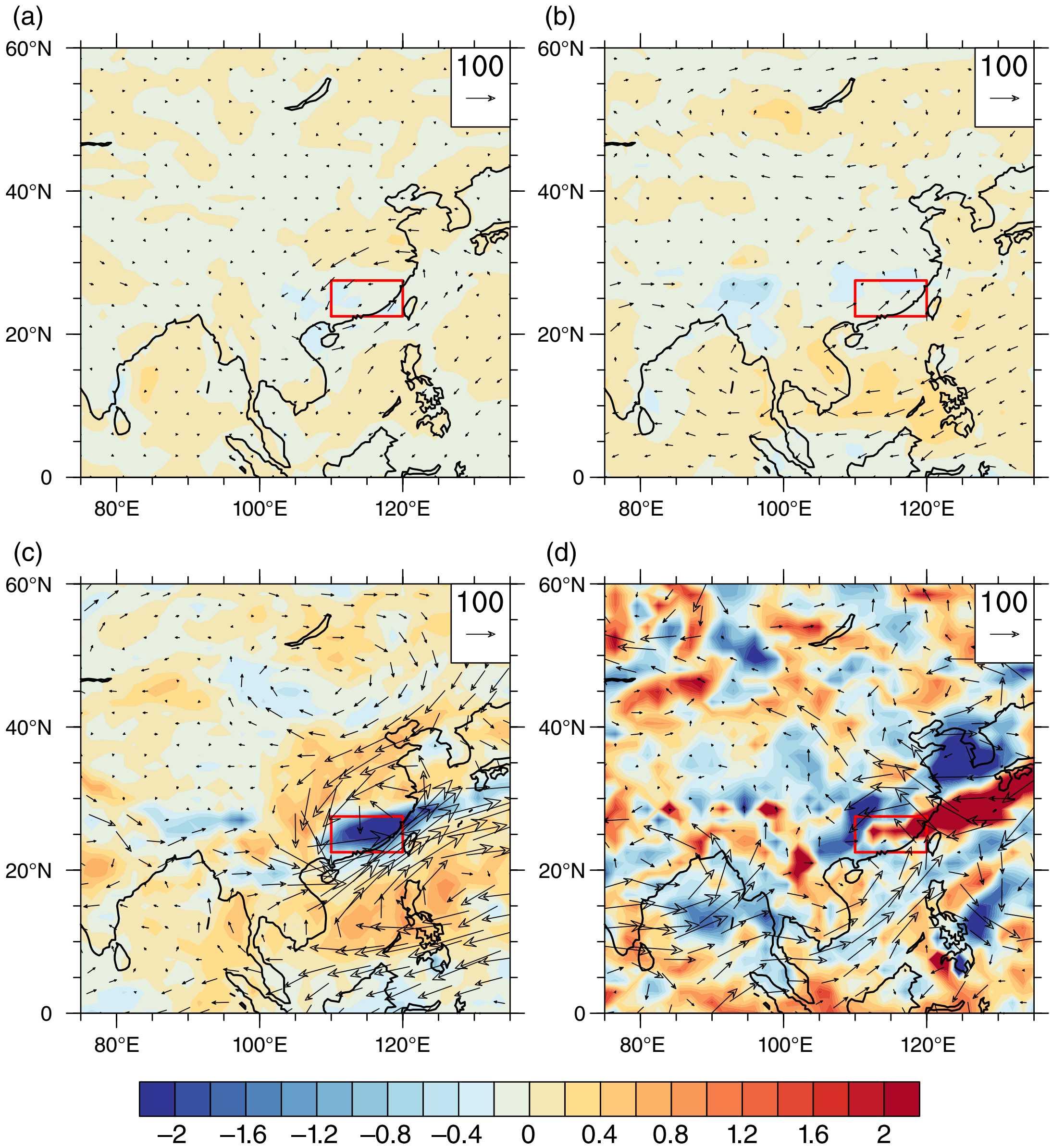

Figure 5. Same as Figure 4 but for the results from ERA-Interim reanalysis during 1979–2010 (the two sub-periods are 1979–1992 and 1993–2010).

analysis further indicates that the increased moisture from the tropical Indian Ocean and the South China Sea in conjunction with the increased convergence after 1992/1993 may have resulted in an obvious increase in clustered extreme precipitation events over SC.

5. Variations in atmospheric stratification

In addition to sufficient moisture, the atmospheric stability is another important factor for the occurrence of extreme precipitation events. Here, the variations in the K index, an integrative indicator of atmospheric stability and moisture, are discussed in the context of clustered extreme precipitation occurrences (Chen *et al.*, 2012a).

First, the regional averaged K value is calculated for 1975–2010 over SC. The results indicate that there is an obvious decadal shift in the K index around 1992/1993, which is concurrent with the variation in the extreme precipitation (figure not shown). Figure 8 shows the spatial distributions of the K anomalies for different periods. Clearly, the K values increased when clustered extreme precipitation events occurred over SC. Correspondingly, a negative anomaly of the vertical velocity in the lower troposphere dominated the region; thus, the upward motion intensified in the lower levels. Furthermore, the K value increased during 1993–2010 compared with 1975–1992.

6. Conclusion

The main characteristics of general extreme precipitation and clustered extreme precipitation events over SC, as well as their associated atmospheric circulations, are explored in this study using station observations and reanalysis data sets. The main conclusions are as follows:

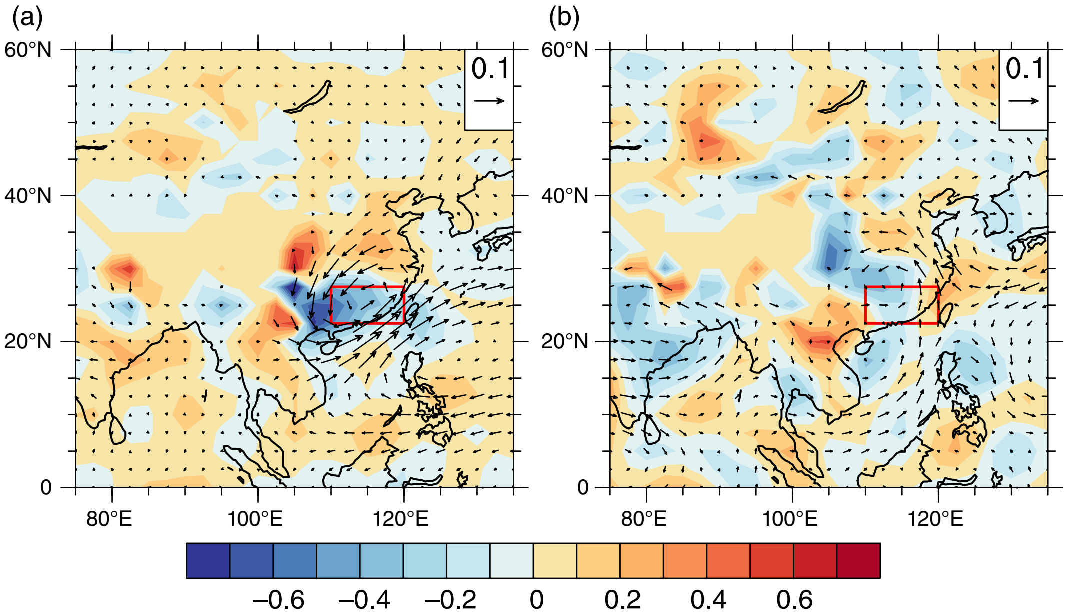

Figure 6. Spatial distributions of WVT anomalies over 850 hPa: (a) anomaly for clustered extreme precipitation during 1975–2010; (b) same as (a) but for the differences between two sub-periods. The units of the wind vectors are m s^{-1}; the units of divergence are 10^{-7} s^{-1}. The red box represents the region of South China.

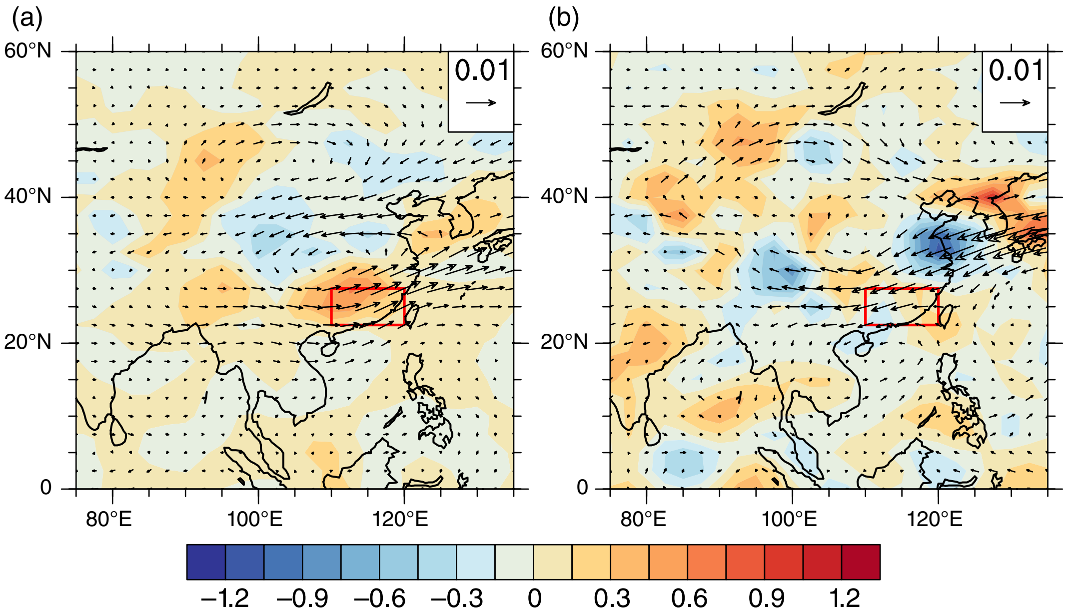

Figure 7. Same as Figure 6 but for 300 hPa; the units of divergence are 10^{-8} s^{-1}. The red box represents the region of South China.

1. Extreme precipitation over SC in summer has undergone a prominent inter-decadal increase since 1992/1993; this finding is concurrent with summer total precipitation. In addition, changes in the frequency and intensity of extreme precipitation played important roles in the corresponding summer total precipitation variations.
2. Obvious changes in the atmospheric circulations can be observed during clustered extreme precipitation events compared with the mean conditions: there was a cyclonic convergence anomaly in the low levels, a southwest movement of the WNPSH in the mid-levels, and a divergence anomaly in the upper levels. These conditions favoured the occurrence of clustered extreme precipitation events over SC. Comparing the differences in the meteorological conditions for the two periods, important results can be obtained: the EAWJ in the upper levels moved northward, the WNPSH in the mid-levels moved eastward, and the low-level airflows from the South China Sea and the North Pacific Ocean intensified during 1993–2010 compared with the airflows during 1975–1992.
3. The results suggest that the integrated WVT of clustered extreme precipitation was reinforced, and

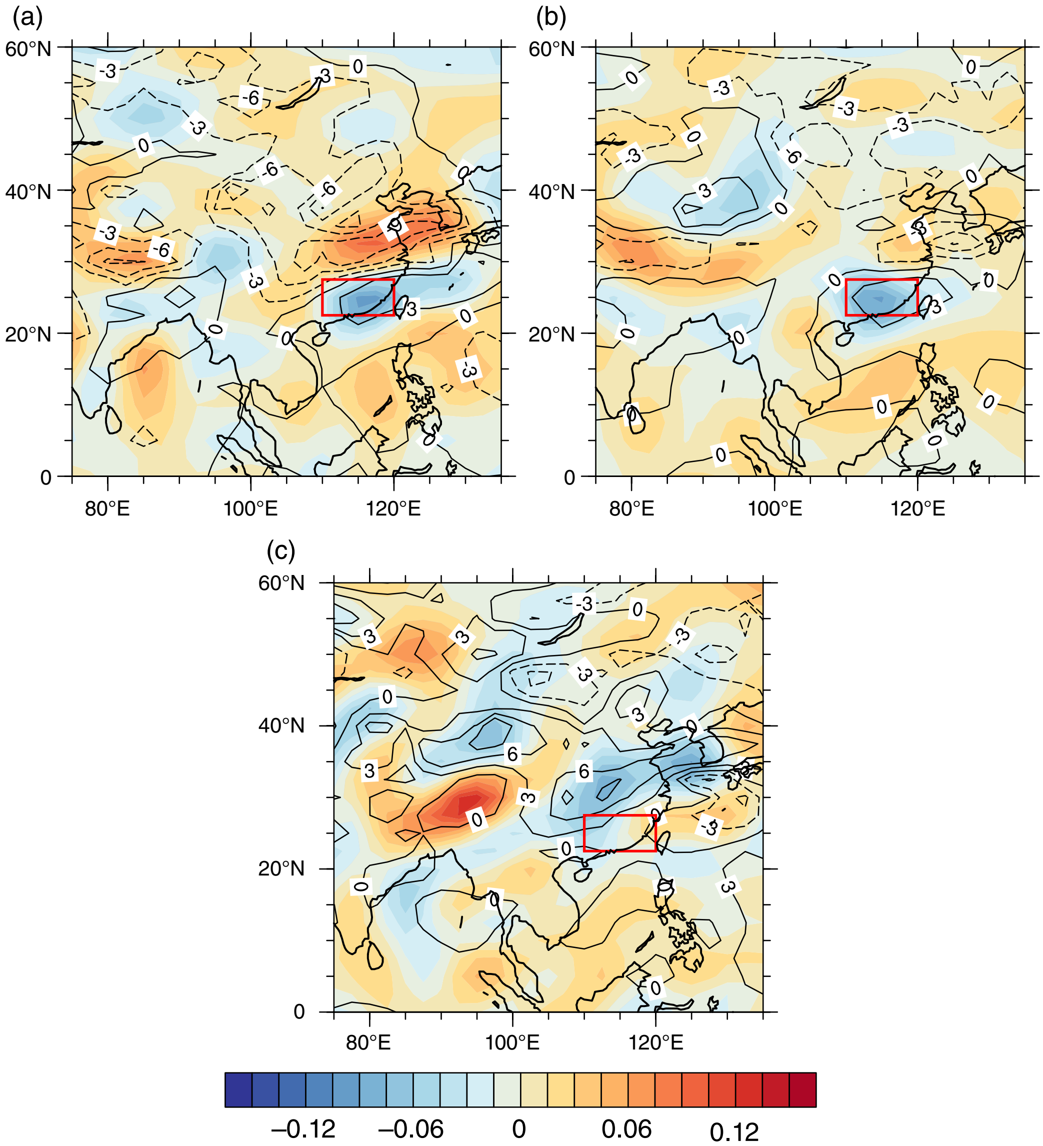

Figure 8. Spatial distributions of the K index and 850 hPa vertical velocity anomalies: (a) differences between clustered extreme precipitation and summer mean during 1975–1992; (b) same as (a) but for the period 1993–2010; (c) differences between two sub-periods for the clustered extreme precipitation events. The colouring indicates the vertical velocity, and the contours indicate the K index. The units of vertical velocity are Pa s^{-1}; the units of the K index are °C. The red box represents the region of South China.

the contribution of each route changed significantly compared with general extreme precipitation. The South China Sea and the Northwest Pacific Ocean were the main enhanced water vapour sources, while the tropical Indian Ocean played a relatively weaker role. For general extreme precipitation events, the WVT branches from the Northwest Pacific Ocean and the tropical Indian Ocean were equally important. In terms of the differences between the two periods, the moisture from the Northwest Pacific Ocean and the South China Sea was reinforced, while the moisture from the tropical Indian Ocean decreased for general extreme precipitation events during 1993–2010 compared with 1975–1992. However, the moisture from the tropical Indian Ocean and the South China Sea was reinforced, while the moisture from the Northwest Pacific Ocean decreased for clustered extreme precipitation events after 1992/1993. These results can be reproduced by ERA-Interim reanalysis data sets which happen to provide a vertically integrated moisture convergence and WVT. Moreover, the WVT had a complex vertical structure.

4. The analysis further shows that when the clustered extreme precipitation events occurred, the unstable atmospheric stratification that enhanced convergence in the low levels and divergence in the upper levels led to a rising motion anomaly over SC. These factors became much stronger after 1992/1993.

Acknowledgements

We sincerely acknowledge the anonymous reviewers whose kind and valuable comments greatly improved the manuscript. This research was jointly supported by the National Natural Science Foundation of China (grant nos. 41210007, 41305061 and 41421004).

References

Chang CP, Zhang YS, Li T. 2000. Inter-annual and inter-decadal variations of the East Asian summer monsoon and tropical Pacific SSTs. Part I: roles of the subtropical ridge. *Int. J. Climatol.* **13**: 4326–4340.

Chen HP, Sun JQ, Chen XL, Zhou W. 2012a. CGCM projections of heavy rainfall events in China. *Int. J. Climatol.* **32**(3): 441–450.

Chen HP, Sun JQ, Fan K. 2012b. Decadal features of heavy rainfall events in eastern China. *Acta Meteorol. Sin.* **26**(3): 289–303.

Ding YH. 2007. The variability of the Asian summer monsoon. *J. Meteorol. Soc. Jpn.* **85B**: 21–54.

Ding YH, Ren GY, Shi GY, Gong P, Zheng XH, Zhai PM, Zhang DE, Zhao ZC, Wang SW, Wang HJ, Luo Y, Chen DL, Gao XJ, Dai XS. 2006. National assessment report of climate change (I): climate change in China and its future trend. *Adv. Clim. Change Res.* **2**(1): 3–8.

Ding YH, Wang ZY, Sun Y. 2008. Inter-decadal variation of the summer precipitation in East China and its association with decreasing Asian summer monsoon. Part I: observed evidences. *Int. J. Climatol.* **28**(9): 1139–1161.

Ding YH, Sun Y, Wang ZY, Zhu YX, Song YF. 2009. Inter-decadal variation of the summer precipitation in China and its association with decreasing Asian summer monsoon Part II: possible causes. *Int. J. Climatol.* **29**(13): 1926–1944.

Du Y, Zhang YC, Xie ZQ. 2008. Impacts of longitude location changes of East Asian westerly jet core on the precipitation distribution during Meiyu period in middle-lower reaches of Yangtze River valley. *Acta Meteorol. Sin.* **66**: 566–576.

Gong DY, Ho CH. 2002. Shift in the summer rainfall over the Yangtze River valley in the late 1970s. *Geophys. Res. Lett.* **29**: 1436–1439.

Han JP, Wang HJ. 2007. Features of inter-decadal changes of the East Asian summer monsoon and similarity and discrepancy in ERA-40 and NCEP/NCAR reanalysis. *Chin. J. Geophys.* **56**: 1666–1676 (in Chinese).

Huang RH, Zhang ZZ, Huang G, Ren BH. 1998. Characteristics of the water vapor transport in East Asian monsoon region and its differences from that in South Asian monsoon region in summer. *Sci. Atmos. Sin.* **22**(4): 460–469 (in Chinese).

Huang RH, Chen JL, Liu Y. 2011. Interdecadal variation of the leading modes of summertime precipitation anomalies over eastern China and its association with water vapor transport over East Asia. *Chin. J. Atmos. Sci.* **35**: 589–606 (in Chinese).

Kwon MH, Jhun JG, Wang B, An S, Kug JS. 2005. Decadal change in relationship between East Asian and WNP summer monsoons. *Geophys. Res. Lett.* **32**(16): 101–120.

Kwon MH, Jhun JG, Ha KJ. 2007. Decadal change in east Asian summer monsoon circulation in the mid-1990s. *Geophys. Res. Lett.* **34**(21): 377–390.

Ning L, Qian YF. 2009. Interdecadal change in extreme precipitation over South China and its mechanism. *Adv. Atmos. Sci.* **26**: 109–118.

Qian WH, Fu JL, Yan ZW. 2007. Decrease of light rain events in summer associated with a warming environment in China during 1961–2005. *Geophys. Res. Lett.* **34**(11): 224–238.

Seager R, Henderson NM. 2013. Diagnostic computation of moisture budgets in the ERA-Interim reanalysis with reference to analysis of CMIP-archived atmospheric model data. *J. Clim.* **26**(20): 7876–7901.

Si D, Ding YH, Liu YJ. 2009. Decadal northward shift of the Meiyu belt and the possible cause. *Chin. Sci. Bull.* **54**: 4742–4748.

Sun B, Wang HJ. 2013. Water vapor transport paths and accumulation during widespread snowfall events in northeastern China. *J. Clim.* **26**(13): 4550–4566.

Sun B, Zhu YL, Wang HJ. 2011. The recent interdecadal and interannual variation of water vapor transport over eastern China. *Adv. Atmos. Sci.* **28**: 1039–1048.

Sun XB, Li QQ, Wei M. 2012. Analysis on interannual and interdecadal variability of annual rainfall over China during 1906-2009. *Meteorol. Mon.* **38**(12): 1464–1472 (in Chinese).

Trenberth KE, Smith L, Qian T, Dai AG, Fasullo J. 2007. Estimates of the global water budget and its annual cycle using observational and model data. *J. Hydrometeorol.* **8**(4): 758–769.

Wang HJ. 2001. The weakening of the Asian monsoon circulation after the end of 1970’s. *Adv. Atmos. Sci.* **18**(3): 376–386.

Wang HJ, Chen HP. 2012. Climate control for southeastern China moisture and precipitation: Indian or East Asian monsoon? *J. Geophys. Res.* **117**: D12109, doi: 10.1029/2012JD017734.

Wang YQ, Zhou L. 2005. Observed trends in extreme precipitation events in China during 1961–2001 and the associated changes in large-scale circulation. *Geophys. Res. Lett.* **32**(9): 297–314.

Wu RG, Wen ZP, Yang S, Li YQ. 2010. An interdecadal change in southern China summer rainfall around 1992/93. *J. Clim.* **23**(9): 2389–2403.

Yang H, Sun SQ. 2005. The characteristics of longitudinal movement of the subtropical high in the western Pacific in the pre-rainy season in South China. *Adv. Atmos. Sci.* **22**(3): 392–400.

Yao C, Yang S, Qian WH, Zheng ML, Min W. 2008. Regional summer precipitation events in Asia and their changes in the past decades. *J. Geophys. Res.* **113**: D17107, doi: 10.1029/2007JD009603.

Zeng G, Sun ZB, Wang WC, Min JZ. 2007. Interdecadal variability of the East Asian summer monsoon and associated atmospheric circulations. *Adv. Atmos. Sci.* **24**(5): 915–926.

Zhai P, Sun AJ, Ren FM, Liu XN, Gao B, Zhang Q. 1999. Changes of climate extremes in China. *Clim. Change*. **42**(1): 203–218, doi: 10.1023/A:1005428602279.

Zhai PM, Zhang XB, Wan H, Pan XH. 2005. Trends in total precipitation and frequency of daily precipitation extremes over China. *J. Clim.* **18**(7): 1096–1108.

Zhang RH. 2001. Relations of water vapor transport from Indian monsoon with that over East Asia and the summer rainfall in China. *Adv. Atmos. Sci.* **18**(5): 1005–1017.

Zhu QG. 2007. *Principle of Synoptic Meteorology*. China Meteorological Press. 344 pp. (in Chinese).

Zhu YL, Wang HJ, Zhou W, Ma HG. 2011. Recent changes in the summer precipitation pattern in East China and the background circulation. *Clim. Dynam.* **36**(7–8): 1463–1473.

